# Supplementary Material

The following document contains supplementary materials in support of the manuscript entitled "A Methodology for Studying the Relationship between Heat Release Profile and Fuel Stratification in Advanced Compression Ignition Engines" by D. DelVescovo, S. Kokjohn, and R. Reitz, submitted to Frontiers of Mechanical Engineering Special Issue: Advancement of Low Temperature Engine Combustion Strategies. For questions or comments, please contact Dan DelVescovo, PhD at delvescovo@oakland.edu.

1   Supplementary Methodology

Figure S.1 shows the trend of equivalence ratio as a function of premixed mass percentage for a condition with a global φ of 0.30, and with 88% of the total fuel mass premixed isooctane, and the remaining 12% direct injected n-heptane for reference. The calculated premixed equivalence ratio was about 0.27, and the local equivalence ratio increased non-linearly with decreasing premixed percentage, and correspondingly increased local DI quantity. The mass of premixed fuel and air defines the background equivalence ratio, while the premixed mass fraction of the zone constrains the local equivalence ratio of the zone.
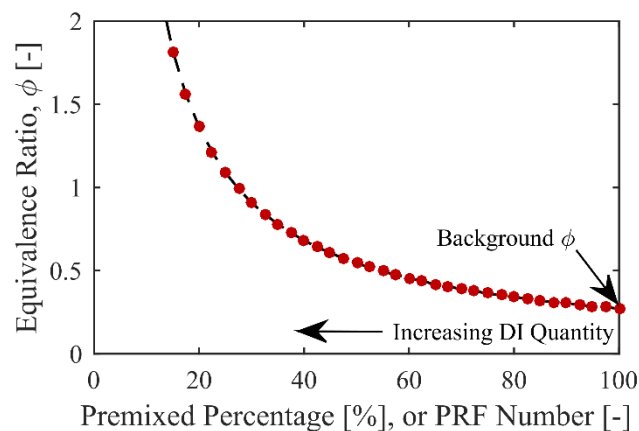

Figure S.1: Local equivalence ratio as a function of local premixed mass percentage or PRF number for a case where premixed fuel is PRF100 and DI fuel is PRF0 with a global φ of 0.30 and 88% premixed fuel
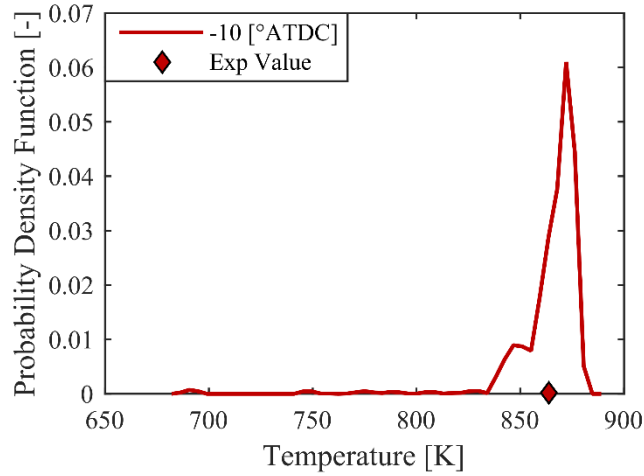
Figure S.2: Example PDF of temperature from non-reacting HCCI simulation at -10 ºCA

Figure S.2 depicts the temperature distribution (presented as a mass-weighted PDF) from a non-reacting CFD simulation for an HCCI combustion simulation utilizing the Caterpillar SCOTE geometry provided in the manuscript. The large high temperature hump is representative of the large piston bowl volume, while the second smaller hump corresponds to the squish volume, where more of the charge is exposed to the firedeck and piston boundaries, and the long tail of the distribution corresponds to the charge trapped in the top ring land crevice region.

An example showing the trend of ignition delay and cumulative autoignition integral is shown in Figure S.3 for 2 mixture compositions (designated by PRF number) where the premixed fuel is iso-octane (PRF100), and the DI fuel is n-heptane (PRF0). As temperature and pressure increases due to compression, the ignition delay decreases and the cumulative AI integral increases until the value of the AI integral reaches 1.0, thus defining the ignition location in crank angle space.
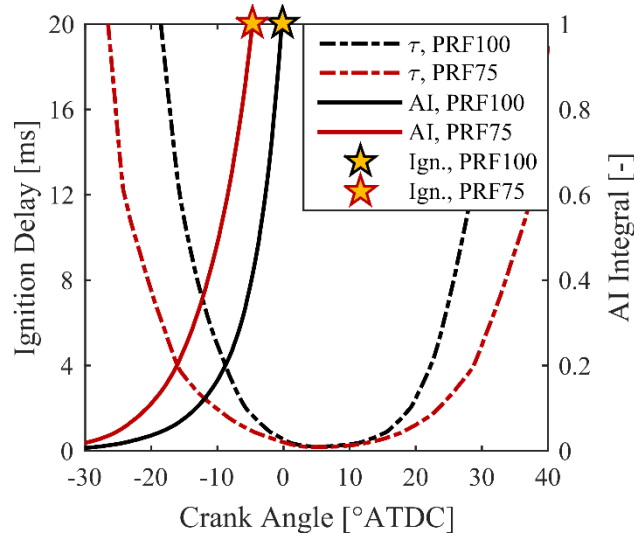
Figure S.3: Ignition delay and cumulative AI integral as a function of crank angle for 2 PRF numbers (PRF100 in black, PRF75 in red) at the mean temperature path, showing the ignition locations (stars). EOI timing is -43 ºATDC

2 Supplementary Validation

Figure S.4 shows the sector mesh used in the 3-D CFD simulations in the present work, while Tables S.1 and S.2 list the initial conditions used in the validation simulations for the HCCI and RCCI cases, respectively, and Figure S.5-S.7 show the comparisons between experimental and CFD predicted pressure and heat release data for the HCCI cases, and the RCCI cases with early SOI timings (-140 to -45 ^{o}ATDC), and late SOI timings (-40 to -17 ^{o}ATDC), respectively.

**Table S.1: Initial conditions of HCCI validation simulations**

Condition	Fuel Mass [mg/cyc]	PRF [-]	P_{IVC} [kPa]	Exp. T_{IVC} [K]	Sim. T_{IVC} [K]
1	58.06	86.6	126.3	354	362
2	58.03	88.6	125.7	354	360
3	58.23	90.1	125.5	352	356

Table S.2: Initial conditions for RCCI validation simulations

| SOI [^{o}ATDC]	Fuel Mass [mg/cyc]	PRF [-]	P_{IVC} [kPa]	Exp. T_{IVC} [K]	Sim. T_{IVC} [K]
-140	58.36	88.4	127.3	351	360
-90	58.55	88.0	127.0	350	358
-60	58.46	88.1	126.4	347	355
-55	58.27	88.4	126.1	346	358
-50	58.48	88.0	126.3	346	355
-45	58.27	88.2	126.3	347	358
-40	58.60	88.0	126.6	348	358
-35	58.46	88.1	127.3	351	358
-30	58.33	88.2	128.0	354	358
-25	58.32	88.1	127.9	353	355
-20	58.49	88.1	127.2	350	350
-17	58.33	88.2	126.7	347	346
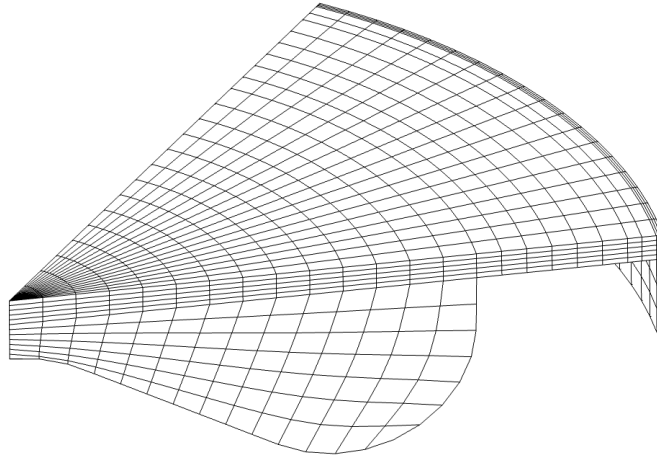
Figure S.4: 51.4º Sector mesh shown at TDC used in 3-D CFD simulations (~10,800 cells)
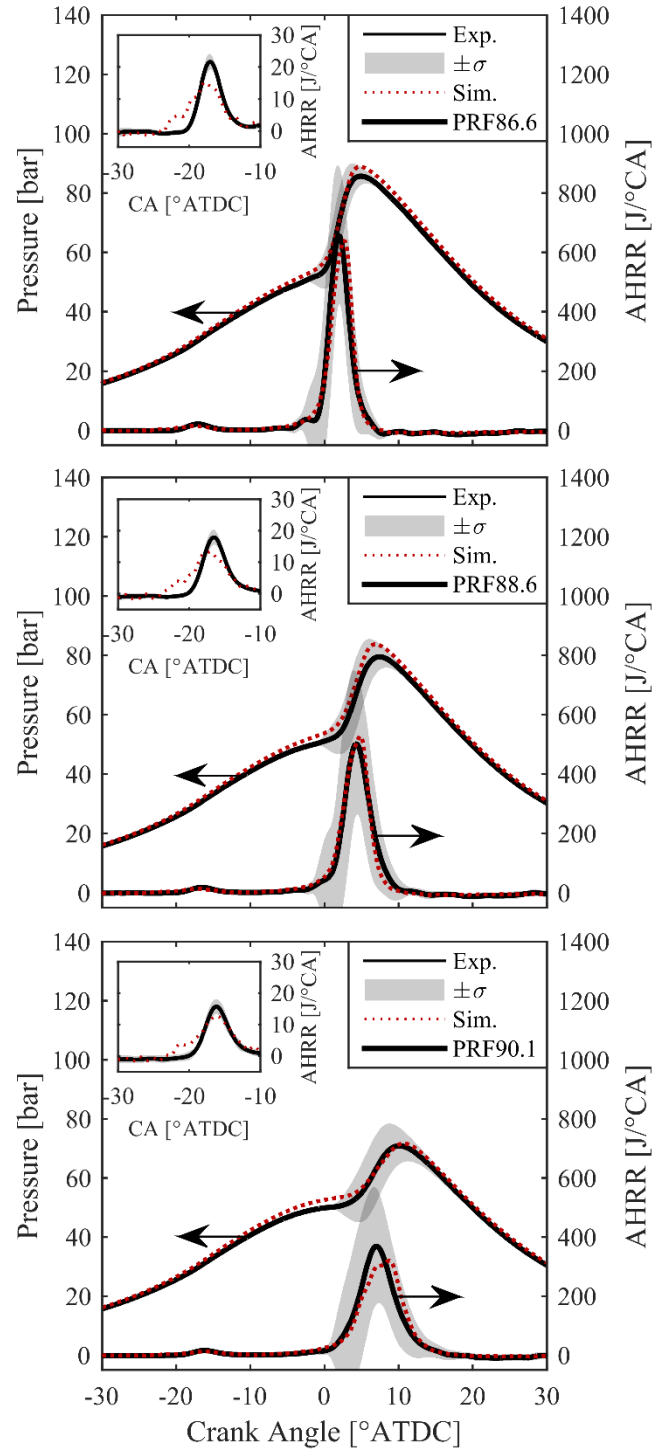
Figure S.5: Comparison of experimental HCCI pressure and heat release rate data (black lines), including standard deviation (grey region) with simulated pressure and heat release rate (red dotted lines) with specified PRF mixture. Inset axis at top left zooms in on low-temperature heat release region
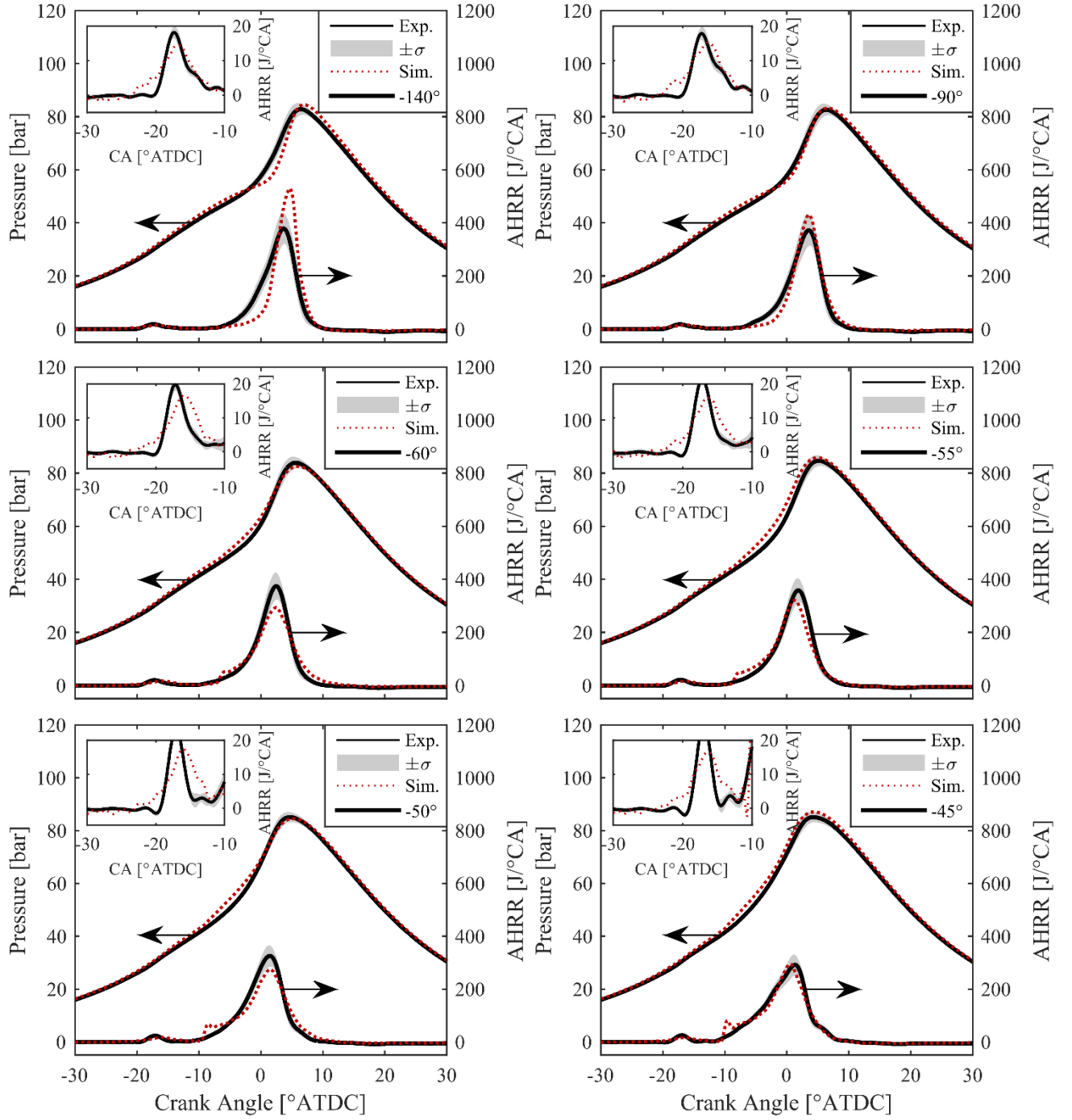
Figure S.6: Comparison of experimental RCCI pressure and heat release rate data (black lines) including standard deviation (grey region) with simulated pressure and heat release rate (red dotted lines) for SOI timing specified in legend (-140º to -45º). Inset axis at top left zooms in on low-temperature heat release region
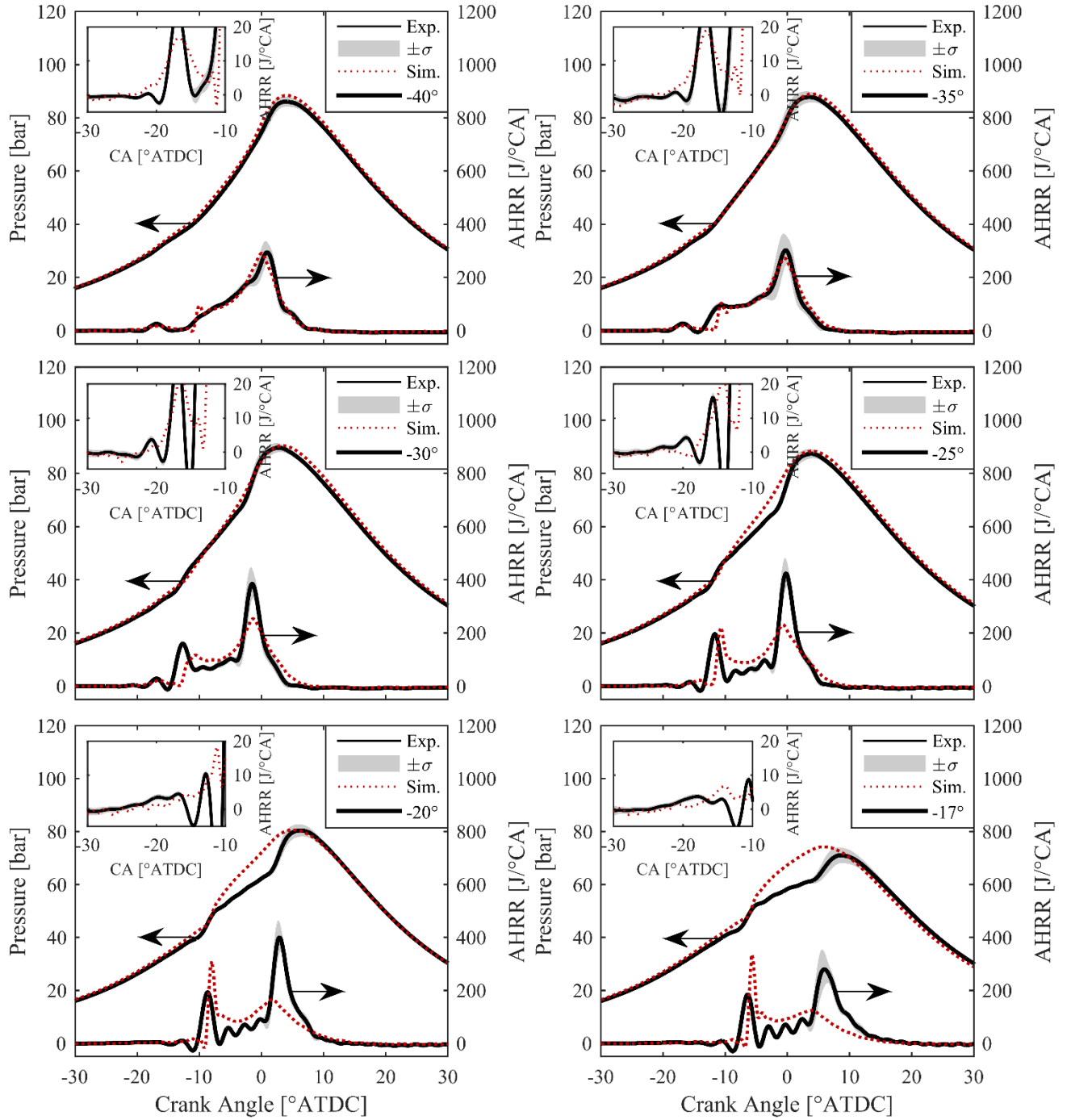
Figure S.7: Comparison of experimental RCCI pressure and heat release rate data (black lines) including standard deviation (grey region) with simulated pressure and heat release rate (red dotted lines) for SOI timing specified in legend (-40º to -17º). Inset axis at top left zooms in on low-temperature heat release region

The standard deviation of temperature parameter (σ_T), was plotted for various SOI timings as a function of crank angle for the non-reacting CFD simulations, and shown in Figure S.8. As can be seen, there is a minor influence on the temperature distribution due to the direct-injected fuel vaporization process, but this effect diminishes over time.
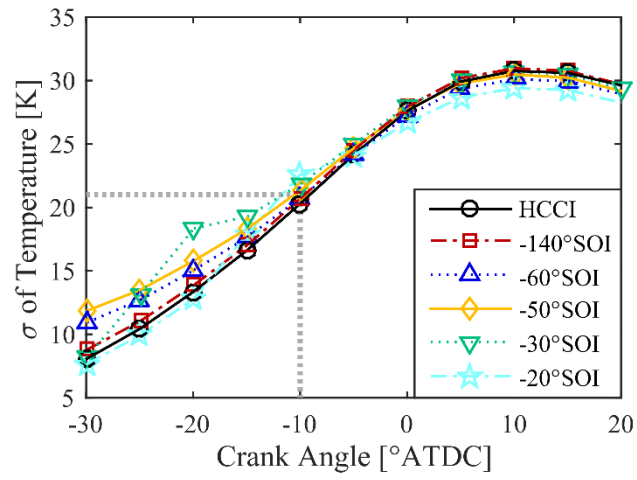
Figure S.8: Standard deviation of temperature as a function of crank angle for various SOI timings with PRF fuels